

## A Broadline NMR Study of the Molecular Motions in Aromatic Polyamides: Poly(*p*-phenylene terephthalamide) and Poly(*m*-phenylene isophthalamide)

Ichiro SUGIYA,<sup>†</sup> Shōdō KOBAYASHI, Shigeo IWAYANAGI,  
and Toshiyuki SHIBATA\*

*Faculty of Technology, Gunma University, Kiryu, Gunma 376, Japan.*

*\*The Institute of Physical and Chemical Research, Wako, Saitama 351, Japan.*

(Received June 16, 1981)

**ABSTRACT:** The anisotropy of the second moment of the proton NMR absorption line was measured at several temperatures on Kevlar and Conex, the fibers of poly(phenylene phthalamide). The curve of the rigid-state second moment with two peaks at  $\omega=0$  and  $90^\circ$  (where  $\omega$  is the alignment angle, *i.e.*, the angle between the fiber axis and the main magnetic field) was calculated for each of these polyamides and found to be in good agreement with the curve measured at  $-150^\circ\text{C}$ . Although the motional narrowing was very slight for Conex [poly(*m*-phenylene isophthalamide)] in the temperature range from  $-150$  to  $+170^\circ\text{C}$ , it was appreciable (*ca.* 2 gauss<sup>2</sup>) for Kevlar [poly(*p*-phenylene terephthalamide)] between  $-50$  and  $+150^\circ\text{C}$ , suggesting the occurrence of the  $180^\circ$  flip-flop motion of the *p*-phenylene rings.

**KEY WORDS** Polyamide / Kevlar / Conex / NMR / Anisotropy / Flip-Flop Motion /

Poly(*p*-phenylene terephthalamide) (abbreviated PpPT) is a well known Kevlar, an ultra high-modulus fiber from E.I. du Pont de Nemour & Co. In an attempt to study the molecular dynamics of this polyamide, the dynamical Young's modulus and the associated mechanical loss were measured by Frosini and Butta<sup>1</sup> and the narrowing of the NMR absorption line by Woodward and Landis.<sup>2</sup> The specimens used, however, were prepared in the laboratory of the former authors and somewhat different from Kevlar. The dynamical mechanical properties obtained by Frosini and Butta were quite different from those obtained on Kevlar later by Haraguchi *et al.*<sup>3</sup>

In this paper, we report the measurements of the second moment of Kevlar fiber as a function of the alignment angle (the angle between the main magnetic field  $H_0$  and the fiber axis) and the temperature. The results on the motional narrowing are shown to be quite different from those of Woodward and Landis.<sup>2</sup> It is shown that the measured

anisotropy of the rigid-state second moment requires that a minor change be made in the crystal lattice given by Northolt and van Arsten.<sup>4</sup> It is further shown that in order to explain the observed temperature dependence of the anisotropy of the second moment, we must assume a thermally stimulated  $180^\circ$  flip-flop motion of the phenylene rings of this aromatic chain polymer. However, no such molecular motion is found in poly(*m*-phenylene isophthalamide) (abbreviated PmPI) from similar NMR measurements.

### EXPERIMENTAL

The specimens used were continuous filament yarns of Kevlar of du Pont (through the courtesy of Dr. Kikuchi of Toray Co.) and single spun yarns of poly(*m*-phenylene isophthalamide), Conex of Teijin Co. (through the courtesy of Dr. M. Yoshino). For the anisotropy measurements, the fibers were aligned in a rectangular cavity bored in a Teflon rod 9 mm in diameter. The temperature dependence of the second moment was measured for isotropic powder specimens obtained by filling the sample

<sup>†</sup> Present address: Kao Soap Co. Ltd., Kayaba-cho 1-1, Nihonbashi, Chuo-ku, Tokyo 103, Japan.

tube with short fibers. All specimens were annealed at 300°C for 24 h *in vacuo* in the sample tube for NMR measurement and then sealed *in situ*.

The NMR spectra were obtained with a broad-line apparatus provided with a Robinson type detector operated at 17 MHz. The radio-frequency magnetic field  $H_1$  was kept as low as possible to avoid saturation. The peak-to-peak modulation amplitude ( $2h_m$ ) was 2 gauss which gave a modulation broadening of  $h_m^2/4=0.25$  gauss<sup>2</sup> in the second moment. The alignment angle  $\omega$  was taken to be zero when the main magnetic field  $H_0$  was parallel to the fiber axis and 90° when  $H_0$  was perpendicular.

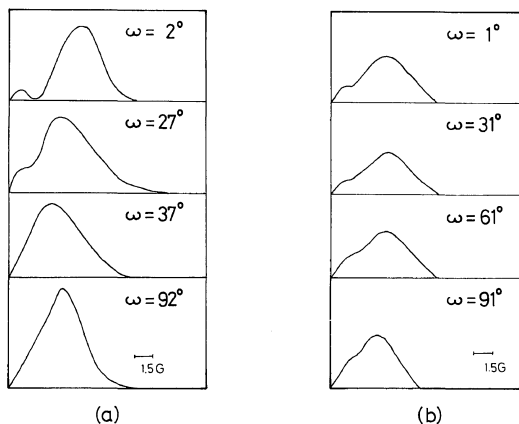


**Figure 1.** Halves of the derivative curves of the NMR absorption line observed at  $-150^\circ\text{C}$  at various alignment angles  $\omega$ . The bars indicate the full modulation amplitude  $2h_m$ : (a) PpPT; (b) PmPI.

## RESULTS

### (i) Line Shape in the Rigid State

Figure 1 shows halves of the derivative curves (as

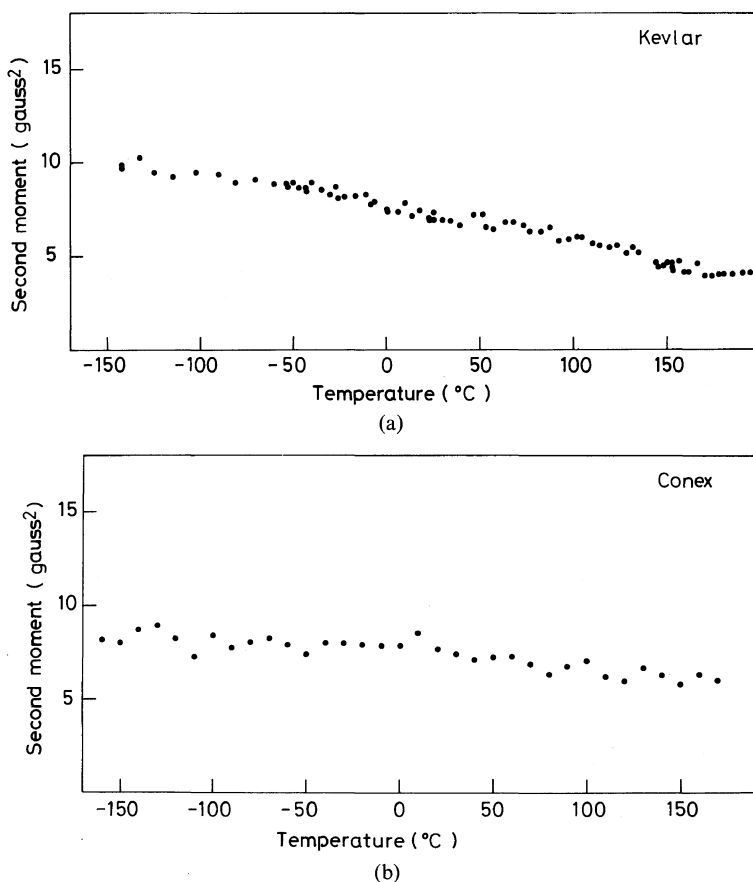


**Figure 2.** Temperature dependence of the second moment of powder specimens: (a) PpPT; (b) PmPI.

recorded on the chart) of the absorption lines of PpPT (a) and PmPI (b) at  $-150^{\circ}\text{C}$  at various alignment angles  $\omega$  indicated. In the upper two curves of Figure 1a for PpPT and in all the curves of Figure 1b for PmPI, a narrow line is seen to overlap the main broad absorption line reminiscent of the two-proton system. This feature is lost from the absorption line for PpPT at larger  $\omega$  (the two lower curves in Figure 1a, at which the main absorption peak is narrowed and overshadows the above-mentioned extremely narrow line. This narrow component of the absorption line is considered to be associated with the water that remains in the specimen after heat treatment. Its intensity is estimated to be very small relative to the total intensity. Therefore, the effect of this narrow-line component is completely neglected in later calculations and discussion.

(ii) *Temperature Dependence of the Second Moment*

Figure 2 shows the temperature dependence of the second moment on "powder" specimens of PpPT (a) and PmPI (b). The lowering of the second moment is seen to be monotonic for both materials. In the rigid state, the space-averaged second moment of PpPT is larger than that of PmPI, due to the difference in the densities of these two isomeric polyamides (1.43 by Northolt<sup>4</sup> and 1.38 g/cm<sup>3</sup> by Kakida *et al.*,<sup>8</sup> respectively). The slight lowering of the second moment with temperature for PmPI may be mainly due to the expansion of the crystal lattice (see DISCUSSION (v)). On the other hand, for PpPT, the lowering is somewhat steeper between  $-50$  and  $+150^{\circ}\text{C}$ , possibly indicating the onset of molecular motions of larger amplitudes to be discussed later.

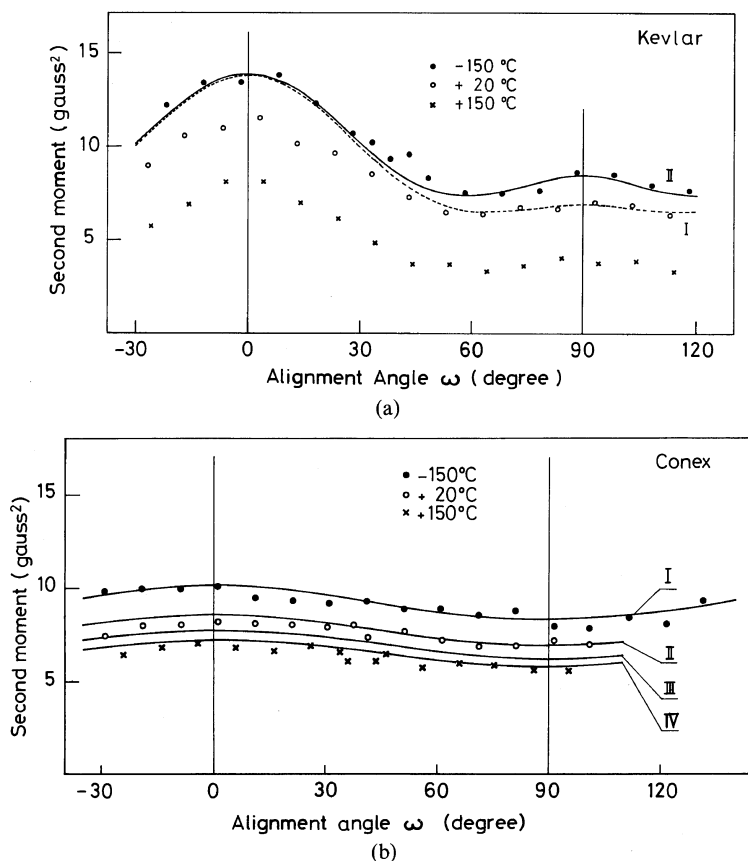


Figure 3. Anisotropy of the second moment  $S(\omega)$  measured at three temperatures indicated. See the text as for the curves I, II, III, and IV: (a) PpPT; (b) PmPI.

(iii) *Anisotropy of the Second Moment*

Figure 3a shows measured second moments of PpPT as a function of  $\omega$  at three temperatures,  $-150$ ,  $+20$ , and  $150^\circ\text{C}$ . The value of  $\omega$  was varied at  $10^\circ$  intervals over the  $140^\circ$  range. The uncertainty of the origin of the alignment angle was corrected by the least squares method, using the general expression for the second moment  $S(\omega)$  of a uniaxially oriented specimen as a function of  $\omega$ ,<sup>5,6</sup>

$$S(\omega) = A \cos^4 \omega - B \cos^2 \omega + C \quad (1)$$

where  $A$ ,  $B$ , and  $C$  are constants.

Two maxima appear in each curve of Figure 3a, one at  $\omega=0^\circ$  is high and the other at  $\omega=90^\circ$  is shallow; both are symmetric about respective centroids. This trend in the anisotropy is opposite to that of the polyoxymethylene crystal<sup>5</sup> obtained by solid-state polymerization of tetraoxane, but similar to that of drawn polyethylene or the polyethylene single crystal.<sup>6</sup> For the polyoxymethylene crystal, only one maximum was observed at  $\omega=45^\circ$  between two deep minima at  $\omega=0$  and  $90^\circ$ . On the other hand, the polyethylene crystal exhibited two maxima at  $\omega=0$  and  $90^\circ$ , the one at  $\omega=90^\circ$  being higher than the other at  $\omega=0^\circ$ . The reversal of the peak height between PpPT and polyethylene has its origin in the fact that the vector of the proton pairs that make a dominant contribution to the second moment is nearly parallel to the fiber axis for PpPT, but perpendicular for polyethylene.

Similar measurements were made on the anisotropy of the second moment of PmPI fiber; the results are shown in Figure 3b. Although the general trend is the same for both fibers, the angular dependence of the second moment is by far less for PmPI than for PpPT. One reason for this difference is the tilting of the crystallites in the PmPI fiber used, as will be discussed later.

## CALCULATIONS AND DISCUSSION

(i) *Calculation of the Second Moment  $S(\omega)$  of PpPT in the Rigid State with Perfect Alignment*

The general procedure for calculating  $S(\omega)$  of a uniaxially oriented specimen was given in our previous report<sup>5</sup> and is a revised version of the modified Van Vleck's expression derived by Olf and Peterlin.<sup>7</sup>

The second moment of a PpPT fiber in the rigid

state was calculated, with the perfect alignment of the fiber axis assumed. The magnetic interactions taken into account were those between 10 protons in the same repeat unit of the polymer and those between them and the protons in the other repeat units within  $7\text{ \AA}$ . Outside this region, protons were assumed to be uniformly distributed. For the contribution from these last protons, the three constants in eq 1 were taken as  $A=B=0$  and  $C=(4/5)\mu^2\pi\rho r_0^{-3}(I+1)/I$ , where  $I=1/2$  for the proton,  $\mu$  is the nuclear magnetic moment of the proton,  $\rho$  is the density of proton in the specimen, and  $r_0$  is the radius of the sphere chosen for the calculation. For PpPT,  $\rho=0.038/\text{\AA}^3$ , and with  $r_0=7\text{ \AA}$ ,  $C$  was found to be  $0.17$  gauss,<sup>2</sup> which is negligibly small. The positions of the 10 protons were determined from the fractional coordinates given by Northolt<sup>4</sup> together with the lattice constants  $a=7.62$ ,  $b=5.21$ , and  $c$  (fiber axis) $=12.59\text{ \AA}$ . The calculation yielded curve I (broken line) in Figure 3a, which is somewhat at variance with the measured second moments at  $-150^\circ\text{C}$ , in particular in the vicinity of  $\omega=90^\circ$ . The lattice constants  $a$  and  $b$  (different from those given by Northolt<sup>4</sup>) used in this calculation were determined from the X-ray photographs at room temperature followed by extrapolation to  $150^\circ\text{C}$ , using the anisotropic thermal expansion coefficient obtained at this laboratory.

A better agreement with the measured second moments was searched by twisting the two successive phenylene rings in a repeat unit about their *para* axes by the angles  $+\phi$  and  $-\phi$  so as to increase the angle between the two rings and/or by rotating the molecule as a whole by an angle  $\Phi$  about the fiber axis from the  $a$ -axis to the  $b$ -axis. Although the rotation of the molecules raises the  $S(\omega)$  curve uniformly, the twisting of phenylene rings lowers the peak centered at  $\omega=0^\circ$  of the  $S(\omega)$  curve without appreciable change in the peak height at  $\omega=90^\circ$ . The curve II in Figure 3a shows the case of  $\phi=3^\circ$  and  $\Phi=-10^\circ$ , the angles being measured from the conformation given by Northolt.<sup>4</sup> The angle of the hydrogen bonding changes by this rotation of the molecules, but the change is not significant. Any reasonable alterations in the bond lengths and angles of protons brought about no favorable results.

(ii) *Effect of the Distribution of the Molecular Axes; the Second Moment of PmPI in the Rigid*

## State

Next, to discuss the distribution of the molecular axes, the distribution function of Gaussian type (normalized to unity),

$$Q(\alpha) = \frac{1}{\sqrt{2\pi}\Delta} \exp(-\alpha^2/2\Delta^2) \quad (2)$$

is assumed to modify the three constants  $A$ ,  $B$ , and  $C$  in eq 1,<sup>5,6</sup> where  $\alpha$  is the angle between the macroscopic fiber axis and the molecular axes (the  $c$ -axes of the constituent crystallites), and  $\Delta$  is a measure of the broadness of the distribution. The constant  $\Delta$  may contain a contribution from the misalignment of the fibers in the sample tube. For a perfect alignment  $\Delta = 0^\circ$ , as was the case for PpPT in (i), and for the isotropic distribution  $\Delta = \infty$ .

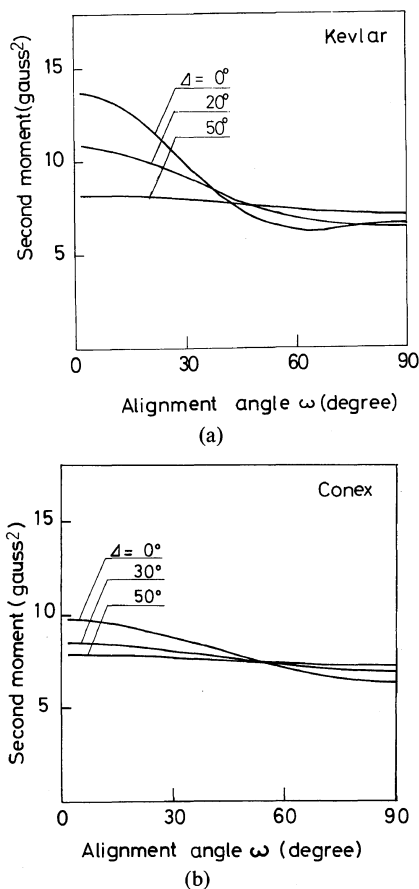


**Figure 4.** Effect of the distribution of the fiber axes on the second moment  $S(\omega)$  at three values of the distribution parameter  $\Delta$ : (a) PpPT; (b) PmPI.

Figure 4 shows the calculated second moments  $S(\omega)$  of PpPT (a) and PmPI (b) for the three values of  $\omega$  indicated. Although no molecular motion was assumed (the rigid state was considered), the lattice constants used were those at room temperature:  $a = 7.87$ ,  $b = 5.18$  and  $c$  (fiber axis) =  $12.9 \text{ \AA}$  for PpPT as given by Northolt,<sup>4</sup> and  $a = 5.27$ ,  $b = 5.25$ ,  $c$  (fiber axis) =  $11.3 \text{ \AA}$   $\alpha = 111.5^\circ$ ,  $\beta = 111.4^\circ$ , and  $\gamma = 88.0^\circ$  for PmPI (triclinic system) as given by Kakida *et al.*<sup>8</sup> Of the three curves for PpPT in Figure 4a, the curve for  $\Delta = 0^\circ$  (not the same as curve I in Figure 3a because of the difference in the lattice constants mentioned) seems to reproduce the measurement best. Thus the perfect alignment ( $\Delta = 0^\circ$ ) assumed in the previous calculation (i) is found to be valid for PpPT.

This is not the case for PmPI as is shown in Figure 4b, where the most appropriate curve for reproducing the measurement is the one corresponding to  $\Delta = 30^\circ$ . By a further investigation, the best fit was obtained when  $\Delta = 28^\circ$ , as shown by the curve II in Figure 3b. This angle of  $28^\circ$  may be taken as the tilt fiber angle for the Conex fiber used in this study. The second moment curve I in Figure 3b that agrees closely with the measured second moment at  $-150^\circ\text{C}$  was obtained with the lattice constants  $a = 5.06$ ,  $b = 5.04 \text{ \AA}$  ( $c$  and the three angles being the same as given above), which were derived by extrapolating Kakida's room temperature values to  $-150^\circ\text{C}$ . In this extrapolation, the thermal expansion coefficient was assumed to be isotropic and  $2.36 \times 10^{-4}/^\circ\text{C}$  for both crystal axes. The isotropic expansion in the  $a$ - $b$  plane of the PmPI crystal is reasonable since hydrogen bonds are formed in both directions; the value of the expansion coefficient, however, is somewhat larger than that expected for hydrogen-bonded polymers.

## (iii) Motional Narrowing in PpPT

The lowering of the second moment with increasing temperature occurs monotonically (Figure 2) and nearly independently of the alignment angle  $\omega$ , *i.e.*, the rigid-state curve (at  $-150^\circ\text{C}$ ) shifts downward at room temperature and  $+150^\circ\text{C}$  without any change in the shape of the curve, as is seen in Figure 3a. The lowering between  $-150^\circ\text{C}$  and room temperature is about 2 gauss,<sup>2</sup> whereas the expansion of the crystal does not contribute more than 0.5 gauss<sup>2</sup> in the same temperature range. There must be some other molecular motion responsible for the

narrowing.

Calculations of the second moment were made on several possible modes of molecular motion to explain the above-mentioned NMR narrowing. In these calculations, all molecular motions were assumed to be statistical oscillations with a full amplitude  $\delta$ . Thus, the molecules were assumed to be found with an equal probability in the range between  $-\delta/2$  and  $+\delta/2$ . Harmonic oscillations would lead to nearly the same conclusion. As examples of calculations that fail to reproduce the measured narrowing, the three modes of oscillation are shown below:

1. The translational oscillation of rigid molecules along the  $a$ -axis without correlation (hydrogen bonds being formed parallel to the  $b$ -axes) (Figure 5);

2. The rotational oscillation of rigid molecules about their long axes with correlation between the molecules (Figure 6);

3. The anti-phase rotational oscillation (both intra and intermolecular) of adjacent phenylene rings with the stationary amide groups connecting them, with the space group symmetry  $P2_1/n$  being maintained (Figure 7).

In each of Figures 5, 6, and 7 are shown only a few curves for clarity; the second moment first increases monotonically with increasing amplitude  $\delta$ ; it goes down to the rigid-state value only when  $\delta$  becomes much larger than  $100^\circ$  (Figures 6 and 7). It

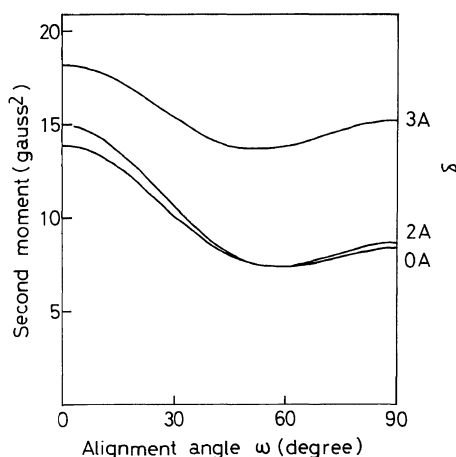


**Figure 5.** Effect of translational oscillations of rigid molecules on  $S(\omega)$  of PpPT calculated at three values of the amplitude  $\delta$ .

was found that this behavior was not affected very much by taking correlations between oscillations into account. In the crystal of PpPT, the molecules are packed so densely and the intermolecular distances are so short that the translation or rotation of the molecules (or part of them) with an appreciable amplitude makes the intermolecular contributions to the second moment large rather than motionally narrowed. Thus, the monotonic narrow-

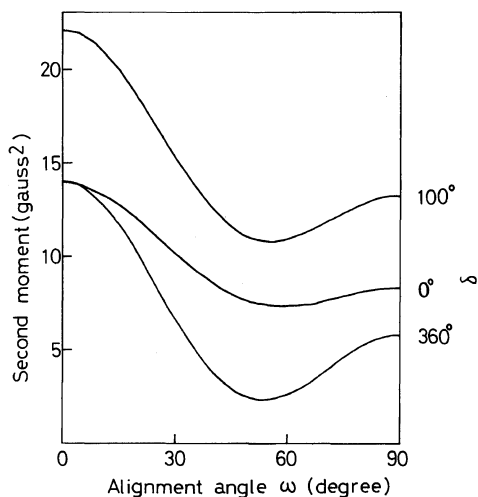


**Figure 6.** Effect of rotational oscillations of rigid molecules on  $S(\omega)$  of PpPT calculated at three values of the amplitude  $\delta$  (with correlation of motions).

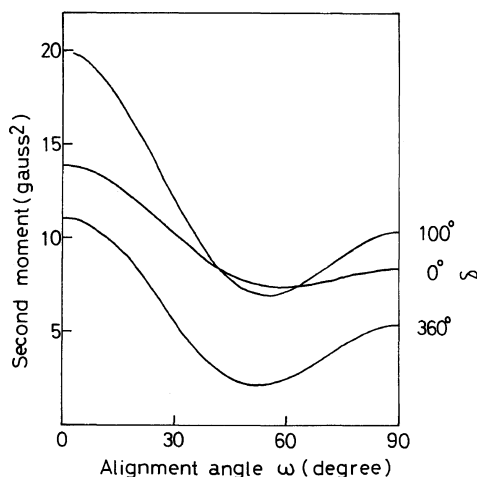


**Figure 7.** Effect of rotational oscillation of phenylene rings on the second moment  $S(\omega)$  of PpPT calculated at three values of the amplitude  $\delta$  (with correlation of motions; see the text).

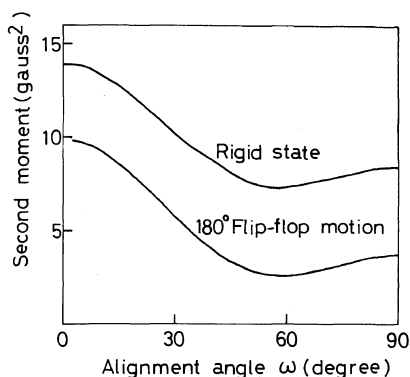


**Figure 8.** The second moment  $S(\omega)$  of PpPT calculated with all phenylene rings in  $180^\circ$  flip-flop motion as compared with  $S(\omega)$  of the rigid state.

ing of the NMR absorption line shown in Figure 2a cannot be explained by progressively increasing amplitudes of oscillations.

#### (iv) Flip-Flop Motion of the Phenylene Rings

It is seen in Figures 6 and 7 that the curve with  $\delta = 360^\circ$  shows an appreciable narrowing. The curve with  $\delta = 360^\circ$  in Figure 6, however, is unfavorable in that at  $\omega = 0^\circ$  the second moment still retains the rigid-state value. Therefore, the rotational oscillation of rigid molecules seems to be ruled out for explaining the narrowing in PpPT. This is consistent with the fact that hydrogen bonds are formed between the amide groups of neighboring molecules.

These considerations lead us to the  $180^\circ$  flip-flop motion of the phenylene rings for interpretation of the motional narrowing observed in PpPT. The lower  $S(\omega)$  curve in Figure 8 was obtained by assuming all the phenylene rings to participate in the  $180^\circ$  flip-flop motion. Correlation between the motions of phenylene rings was found to be not essential for the calculation. The most important in Figure 8 is that the curve for the  $180^\circ$  flip-flop motion is nearly parallel to the rigid-state curve, which is an outstanding feature of the narrowing observed in Figure 3a.

The observed narrowing in Figure 2a, though gradual in the whole range of temperature, is somewhat steeper in the temperature range from  $-50$  to  $+150^\circ\text{C}$  than elsewhere. We can attribute the NMR narrowing in this temperature range to the thermally stimulated  $180^\circ$  flip-flop motion of the phenyl-

ene rings. Thus, the number of the phenylene rings that are excited to a flip-flop frequency ( $\approx 10^5$  Hz) necessary for the motional narrowing increases gradually with increasing temperature. It should be noted that this temperature range is a little higher than the range in which Haraguchi *et al.*<sup>3</sup> observed a  $\beta$  mechanical loss at lower frequencies. These authors attributed this loss to molecular motions in the amorphous part of the polymer. In our calculation of  $S(\omega)$ , however, the specimen was assumed to be 100% crystalline; this assumption would not be serious, since the non-crystalline part would contribute to  $S(\omega)$  as much as the crystalline part does, if it is in the rigid state.

The flip-flop motion may be justified from the barrier heights for the rotation of phenylene rings

on both sides of the amide group  $\begin{array}{c} \text{O} \\ \parallel \\ -\text{N}-\text{C}- \\ | \\ \text{H} \end{array}$ . A value as

high as 12 kcal/mol for the rotation was reported by Tadokoro *et al.*,<sup>9</sup> who for the first time made an empirical conformational energy calculation for PpPT. Later, relatively low values were reported in the conformational energy calculation by Lauprêtre and Monnerie,<sup>10</sup> who used PCILO (Perturbative Configuration Interaction using Localized Orbitals) program. Although the energy barrier about the  $\text{C}_{\text{AR}}-\text{N}$  bond was still high ( $9 \text{ kcal mol}^{-1}$ ), that about  $\text{C}_{\text{AR}}-\text{C}_{\text{AMIDE}}$  bond was as low as  $2 \text{ kcal mol}^{-1}$ , suggesting that the rotation about the latter bond is much easier than that about the former bond. Thus, the flip-flop motion will be realized more easily than anticipated, at least, in one half of the phenylene rings in PpPT.

#### (v) Motional Narrowing in PmPI

The second moment of PmPI shown in Figure 3b as curve III was calculated with the lattice constants  $a = 5.43$  and  $b = 5.41 \text{ \AA}$ , which were found by extrapolating from room temperature to  $+150^\circ\text{C}$  using the thermal expansion coefficients given previously. This curve appears above the measured second moment. Therefore, some molecular motions must be assumed at temperatures higher than room temperature. For explaining the narrowing in PmPI, several modes of motions were tested. Though the details of the calculation are not shown here, PmPI was found to behave very differently from PpPT. Thus, as the amplitude  $\delta$  of oscillations was increased, the second moment of PmPI at first was

decreased definitely and then increased at moderately large amplitudes. The curve IV in Figure 3b is the second moment calculated for the rotational oscillation of rigid molecule with  $\delta=35^\circ$  assumed and is seen to reproduce well the measured values at  $+150^\circ\text{C}$ . More complex modes of motions will be needed to explain the observed narrowing completely, but the amplitude  $\delta=35^\circ$  is not unexpected for (parts of) ordinary chain polymers in crystalline state. It is interesting that the motional narrowing differs so much between the two isomeric polyamides: poly(*m*-phenylene isophthalamide) and poly(*p*-phenylene terephthalamide). In the former, the flip-flop motion of the phenylene rings is not possible owing to the lack of symmetry and, instead, oscillational motions of moderate amplitude are expected to occur more easily than in the latter.

In conclusion, the flip-flop motion of phenylene rings seems to occur only about *para* axes of the rings in chain polymers with an appreciable rigidity. Up to date, no evidence of the flip-flop motion has been observed in aromatic polymers other than poly(*p*-phenylene terephthalamide) investigated here.

*Acknowledgment.* This work was partially supported by the Grant-in-Aid for Scientific Research from the Ministry of Education, Science and Culture of Japan. We thank Dr J. Uzawa of the Institute of Physical and Chemical Research for the NMR measurements. Thanks are due to Professor

R. Chûjô of the Tokyo Institute of Technology for his comments on the possibility of the flip-flop motion.

## REFERENCES

1. V. Frosini and E. Butta, *J. Polym. Sci., A-2*, **9**, 253 (1971).
2. A. E. Woodward and J. Landis, *J. Polym. Sci., Polym. Phys. Ed.*, **10**, 2051 (1971).
3. K. Haraguchi, T. Kajiyama, and M. Takayanagi, *Rep. Prog. Polym. Phys. Jpn.*, **XIX**, 303 (1976).
4. M. G. Northolt and J. J. van Arsten, *J. Polym. Sci., Polym. Lett. Ed.*, **11**, 333 (1973); M. G. Northolt, *Eur. Polym. J.*, **10**, 799 (1974).
5. T. Shibata and S. Iwayanagi, *Polym. J.*, **10**, 599 (1978).
6. H. G. Olf and A. Peterlin, *J. Polym. Sci., A-2*, **8**, 771 (1970).
7. H. G. Olf and A. Peterlin, *J. Polym. Sci., A-2*, **8**, 753 (1970).
8. H. Kakida, Y. Chatani, and H. Tadokoro, *J. Polym. Sci., Polym. Phys. Ed.*, **14**, 427 (1976).
9. K. Tashiro, M. Kobayashi, and H. Tadokoro, *Macromolecules*, **10**, 413 (1977).
10. F. Lauprêtre and L. Monnerie, *Eur. Polym. J.*, **14**, 415 (1978).

## ERRATUM

For the fifth equation of eq (A-7) in ref 5 read

$$G_5 = \langle \sin^2 \gamma_{i,j} \sin 2 \phi_{i,j} / r_{i,j}^3 \rangle t$$

The calculation of ref 5, nevertheless, has not suffered from this error in typewriting.